

Membrane mediated aggregation of curvature inducing nematogens and membrane tubulation

N. Ramakrishnan* and P. B. Sunil Kumar†

Department of Physics, Indian Institute of Technology Madras, Chennai 600036, India

John H. Ipsen‡

*MEMPHYS- Center for Biomembrane Physics, Department of Physics and Chemistry,
University of Southern Denmark, Campusvej 55, DK-5230 Odense M, Denmark*

(Dated: September 30, 2018)

Abstract

The shapes of cell membranes are largely regulated by membrane associated, curvature active, proteins. We use a numerical model of the membrane with elongated membrane inclusions, recently developed by us, which posses spontaneous directional curvatures that could be different along and perpendicular to its long axis. We show that, due to membrane mediated interactions these curvature inducing membrane nematogens can oligomerize spontaneously, even at low concentrations, and change the local shape of the membrane. We demonstrate that for a large group of such inclusions, where the two spontaneous curvatures have equal sign, the tubular conformation and sometime the sheet conformation of the membrane are the common equilibrium shapes. We elucidate the factors necessary for the formation of these *protein lattices*. Furthermore, the elastic properties of the tubes, like their compressional stiffness and persistence length are calculated. Finally, we discuss the possible role of nematic disclination in capping and branching of the tubular membranes.

PACS numbers: PACS-87.16.D-, Membranes, bilayers and vesicles. PACS-05.40.-a Fluctuation phenomena, random processes, noise and Brownian motion. PACS-05.70.Np Interfaces and surface thermodynamics

arXiv:1302.1641v1 [physics.bio-ph] 7 Feb 2013

*Electronic address: ram@physics.iitm.ac.in

†Electronic address: sunil@physics.iitm.ac.in

‡Electronic address: ipsen@memphys.sdu.dk

I. INTRODUCTION

Membrane shape deformations are key phenomena in a multitude of cellular processes, including protein sorting, protein transport, organelle biogenesis and signaling. In the last decade a profusion of regulatory proteins facilitating such shape changes of the cellular membranes has been unravelled, with the BAR protein superfamily [1], the Pex11 family [2] and coat proteins [3] as notable examples. The possibility of such mechanisms has long been anticipated in the biophysical literature [4, 5]. However the experimental and theoretical difficulties involved have hampered the establishment of a quantitative basis for interpreting such phenomena in cell biology. Recently, we had overcome one such obstacle by the establishment of a computer simulation technique to study how the cooperative effects of membrane inclusions, imposing a curvature along the direction of its orientation, remodels vesicular membranes [6].

In this work we aim at describing, from a theoretical point of view, the effect of a large group of these membrane curving proteins, which can be considered as effectively elongated objects in the plane of the membrane. We consider inclusions with approximate π -symmetry, i.e. the protein can be considered as essentially indistinguishable from its form rotated by 180° around the protein center in the plane of the membrane. The membrane inclusions we consider, has thus some similarity with nematogens in 3-D nematic liquid crystals. However, they are embedded in a membrane and may couple to its geometry, and it is only the part of the protein in contact with the membrane, which will be subject to these symmetry requirement. Therefore, we cannot consider these membrane inclusions as simple liquid crystal nematogens restricted to Euclidean two dimensional surfaces. In the following we will refer to such membrane inclusions as membrane nematogens. Large groups of membrane curving proteins fall into this category of membrane nematogens. An example is the BAR proteins (proteins containing both BAR domains and/or N-terminal helices), where both the N-terminal amphipathic helices and the banana-shaped, positively charged, dimeric interface with the membrane, induces directional curvature [7–12]. The caveolin protein family [13], which form dimers and are bound to the membrane by a pair of hairpins and the reticulon, DP1 and Yop1p involved in the formation of smooth ER [15, 16], and are anchored to the membrane by two similar hairpins are also examples. The cell biology literature has provided good evidence for that the insertion of amphipathic helical peptide sequences not only provide a binding mechanism, but also gives rise to local modulation of the membrane curvature [17, 18]. More solid, quantitative support for this conjecture is given from biophysical experiments [19] and theory [20]. Furthermore, biophysical studies has demonstrated that curvature active membrane inclusions have dramatic effects on the cooperative behavior with a complex interplay between lateral ordering and membrane shape. However, the detailed mechanisms leading to the specific complex membrane-protein structures have not been characterized. This work will elucidate some aspects of these mechanisms for the membrane nematogens.

Some of the key processes involved in the structural organization of membrane nematogens described in the cell biology literature, can be categorized as follows: (1) the aggregation of the nematogens - the process where membrane proteins upon activation and/or binding to the membrane spontaneously aggregate and form functional cluster of proteins in the membrane [9–11, 14], (2) Tubulation of membranes, where the aggregate and the membrane develop tube-like membrane structures (e.g. sorting endosomes [21, 22] and Mitochondrial outer membrane [23], formation of T-tubules in *Drosophila* [24]) and (3) The formation of *protein lattices*, often characterized by helical arrangement of the proteins spiraling around the tubular membrane, e.g. for dynamin [25, 26] or caveolin [27].

In this work, we will demonstrate by numerical analysis of a possible physical model, which captures the membrane conformations and the organization of in-plane nematogens, that the above mentioned processes directly results from the cooperative thermodynamic behavior of the nematogens coupled to the flexible membrane. Also, we will discuss aspects of the stability of membrane tubes and the formation of the edges for membrane sheets. Our model gives a coarse description of the membrane, which capture properties of the membrane which are essential for its large scale organization. Despite the simplicity of the model, the parameter space is too large for a comprehensive discussion of its phase behavior. Rather, we will focus on some generic features of the model which may well give a framework for interpreting the experimental observations of cellular membrane morphogenesis. Previously, protein induced membrane tube formation has been considered by a phenomenological model involving scalar fields [28], and the coupling between membranes and inclusions with directional curvature was modelled in [29–32].

The paper is organized as follows: In Section II the physical model of the interacting system of membrane and membrane nematogens are presented, while details about the numerical analysis is given in **Supplementary Materials**. Section III on **Results and Discussion** present some generic properties of

the model and discuss their possible relevance to experimental results. In section III A-III C the aggregation of proteins and membrane domain formation, membrane tubulation and formation of *protein lattices* are described in the framework of the model. Section III D discusses the elastic properties of membrane tubes and their relevance to observable effects. Much of the characterization of the elasticity of *protein lattices* is based on a continuum version of the model discussed **Supplementary Materials**. Section III E discusses mechanisms of closing, capping and branching of membrane tubules and the possible role of nematic point defects. Section III F describes aspects of the stability of membrane tubules with more membrane curvature components. In section III G the interplay between sheet and tubule formation is described and possible implications for cell organel morphology is discussed. Some perspective on the modeling of membrane morphogenesis is given in **Conclusion**, Section IV. We will in this work specialize to properties of membranes with inclusions which possess directional curvatures of equal sign. We will consider cases with different signs of the directional curvatures in a separate publication.

II. MODEL

The modeling of the effects of in-plane nematogens on membrane structure, will in this work, be treated with a discretized description of the surface as a randomly triangulated mesh. A continuous surface conformation is approximated by a collection of triangles glued together to form a closed surface of well defined topology. A triangulated surface, with spherical topology, thus consist of N vertices connected by $N_L = 3(N - 2)$ links, which enclose $N_T = 2(N - 2)$ triangles. Each vertex v is assigned a position \vec{X}_v . This tessellations of the surface form the basis for a coarse grained description of the membrane, where only the gross features of the structure and interactions are important.

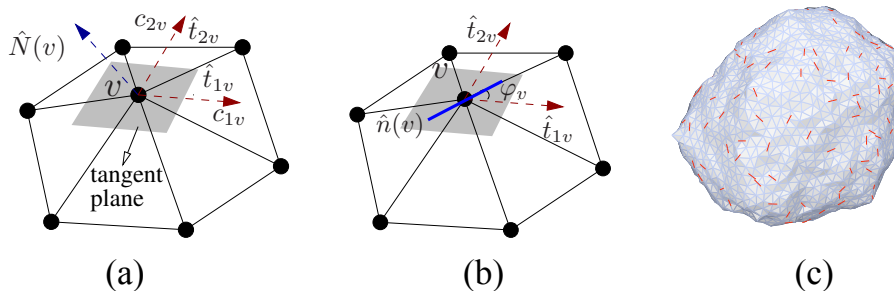


FIG. 1: (a) A one ring triangulated patch around a vertex v . The shaded region represents the tangent plane at v and $\hat{N}(v)$ its corresponding normal. c_{1v} and c_{2v} are the maximum and minimum principal curvatures, respectively, along principal directions \hat{t}_{1v} and \hat{t}_{2v} . (b) Illustration of the nematic field vector \hat{n} defined on the tangent plane of vertex v . (c) A vesicle of spherical topology with spatially random surface nematogens.

The triangulation and the vertex position form together a discretized surface, a patch of which is given in fig:???. The geometry of the continuous surface, which is approximated by the triangulated surface, can now be characterized by a number of surface quantifiers, e.g. the curvature tensor, the principal directions (\hat{t}_{1v} & \hat{t}_{2v}), the corresponding principal curvatures (c_{1v} & c_{2v}) and surface normal, $\hat{N}(v)$, at each vertex v . The details can be found in [6]. The discretized Helfrich's free energy[34] can then be evaluated as

$$\mathcal{H}_c = \frac{\kappa}{2} \sum_{v=1}^N \frac{A_v}{3} H_v^2 \quad (1)$$

where $H_v = (c_{1v} + c_{2v})/2$ the mean curvature at vertex v and A_v is the area of the surface patch occupied by the triangles adjacent to vertex v . κ is the bending rigidity of the membrane. Furthermore we are in a position to calculate the directional curvatures along and perpendicular to a unit vector \hat{n} along the surface by use of Gauss formula:

$$\begin{aligned} H_{v,\parallel} &= c_{1v} \cos^2 \varphi_v + c_{2v} \sin^2 \varphi_v, \\ H_{v,\perp} &= c_{1v} \sin^2 \varphi_v + c_{2v} \cos^2 \varphi_v, \end{aligned} \quad (2)$$

where φ_v is the angle between \hat{n} and the principal direction \hat{t}_{1v} . Such an orientational spontaneous curvature may be induced by a membrane nematogen with an orientation in the plane of the membrane given by \hat{n} . In addition to the interaction with the membrane, nematogens may tend to orient along each other at close proximity due to steric, electrostatic and dispersion interactions [35]. In the present study, we focus only on the two dimensional orientational interactions promoted by the underlying, non-planar, fluctuating membrane [36–40]. The π -symmetry of the individual nematogens dictates that the simplest form of their self interaction should be of the type $\cos^2(\theta_{vu})$ and $\sin^2(\theta_{vu})$, where θ_{vu} is the angle between \hat{n}_v and \hat{n}_u at neighboring vertices. We choose to represent the interactions between membrane nematogens by an extension of the well-established Lebwohl-Lasher model of nematic ordering in presence of vacancies, here implemented on a triangulated surface model of a membrane.

The nearest neighbor interaction between the nematogens is composed of an isotropic component represented by an interaction strength J and an anisotropic (quadrupolar) correction measured by the interaction constant ϵ_{LL} . The total interaction between the membrane nematogens thus takes the form

$$\mathcal{H}_{\text{field}} = \sum_{\langle vu \rangle} \left\{ -\frac{J}{2} - \epsilon_{LL} \left(\frac{3}{2} \cos^2(\theta_{vu}) - \frac{1}{2} \right) \right\} I_v I_u, \quad (3)$$

where the sum is over nearest neighbour vertices. $I_v = 0, 1$ is an occupation variable, which is unity if vertex "v" is occupied by a nematogen and zero if otherwise. The calculation of the θ_{vu} is non-trivial, since the angle between spatially separated nematogens are measured after the parallel transport of vectors along the curved surface [6]. With this measure of the angular differences, Eq.(3) models the in-plane interactions of the nematogens mediated by the membrane. The direct distance dependent interactions through the cytosol is not taken into account in this model of membrane-protein conformations. Sufficiently large, positive ϵ_{LL} favors in-plane ordering of the nematogens. The effect on the anisotropic elasticity of the membrane due to the nematogens, in analogy with the discretized Helfrich free energy, takes the form [6]:

$$\mathcal{H}_{nc} = \sum_{v=1}^N \left\{ \frac{\kappa_{\parallel}}{2} (H_{v,\parallel} - H_{\parallel}^0)^2 + \frac{\kappa_{\perp}}{2} (H_{v,\perp} - H_{\perp}^0)^2 \right\} I_v A_v \quad (4)$$

H_{\parallel}^0 and H_{\perp}^0 are the spontaneous curvatures along \hat{n} and \hat{n}^{\perp} , while κ_{\parallel} and κ_{\perp} are the corresponding directional membrane bending elastic constants.

Self avoidance of the discretized surface is ensured by imposing constraints on the neighboring vertex distance and on the dihedral angles between neighboring faces[6]. The equilibrium properties of the discretized surface can now be evaluated by standard Monte Carlo sampling of Boltzmann's probability distribution $\sim \exp\left(-\frac{1}{k_B T}[\mathcal{H}_c + \mathcal{H}_{\text{field}} + \mathcal{H}_{nc}]\right)$ at fixed concentrations of the membrane nematogens. A general description of the implementation of such numerical models and further details about the simulations are given in [6].

Finally, we will make some considerations about length scales. The lattice model is a highly coarse-grained representation of the membrane, designed to capture the large length-scale properties of membranes with inclusions. Therefore, the triangulated surface represent a collection of membrane patches with a characteristic length scale. A natural choice of length scale is to identify a tether length with the lateral extension of a membrane inclusion. Some examples here are CIP4 F-BAR with a length of 22 nm[41] or dynamin which extent about 25 nm [25].

The computer simulations of the discrete model provide us with insight into the nature of equilibrium configurations for a choice of model parameters. To complement the numerical simulations, it is useful to consider the corresponding continuum model in the limit of membrane nematogen with 100% surface coverage. It is an extension of Helfrich's bending free energy functional [42, 43]

$$\mathcal{F} = \oint dA \left\{ \frac{K_A}{2} \text{Tr}(\nabla \hat{n} : \nabla \hat{n}) + \frac{\kappa}{2} (2H)^2 + \frac{\kappa_{\parallel}}{2} (H_{n,\parallel} - H_{\parallel}^0)^2 + \frac{\kappa_{\perp}}{2} (H_{n,\perp} - H_{\perp}^0)^2 \right\}$$

where $K_A = \frac{3\sqrt{3}}{2}\epsilon_{LL}$. In **Supplementary Material** is presented such an analysis of the mechanical properties of a tubular membrane with a protein coat and analytical expressions reflecting, tube radius, persistence length and protein organization are also derived.

III. RESULTS AND DISCUSSION

In this section we will present some key aspects resulting from the coupling of membrane nematogen proteins to lipid membranes. It will both contain results from computer simulations of the aforementioned model, which are non-perturbative, along with theoretical analysis of the continuum model, of a more perturbative character to qualify the numerical finding. Throughout the discussion the parameter ϵ_{LL} has a relatively high value (several $k_B T$ in a range where nematic ordering is favored). Furthermore, the implications of our results on the experimental systems *in vivo* and *in vitro* will be discussed.

A. Aggregation and membrane domain formation of membrane nematogens

A common feature of membrane nematogens is their strong tendency to self-associate, driven by the flexible geometry of the membrane - in this manuscript, we call this self associated structure to be an aggregate or a domain. Self association has been observed for a wide range of model parameters κ_{\parallel} , κ_{\perp} , H_{\parallel}^0 and H_{\perp}^0 . All results presented in the following corresponds to system size with $N = 2030$ vertices. When the fraction of nematogens $\phi_A = 0.3$, $\epsilon_{LL} = 3$ and $J = 0$ (in units of $k_B T$), the flexible membrane with curvature coupled to the nematic orientation, gives rise to co-existence of nematically ordered domains and the isotropic dilute phase, this is shown in figure-2(b). This is to be compared with the planar Lebwohl-Lasher model on a random triangular lattice, at the same concentration, where the isotropic phase is stable (see Supplementary Materials). Additional direct repulsive interactions $J \leq -0.5$ between the membrane nematogens can reestablish the isotropic phase, which is shown in Fig. 2(a). The aggregation of membrane nematogens cause shape deformation of the whole membrane with the collective involvement of all the degrees of freedoms, lateral orientation, lateral position and membrane conformation. In general the lateral domain formation depends on all the involved parameters - e.g. increasing J promotes the aggregation and can change the aggregate shape as shown in Fig. (2)(c).

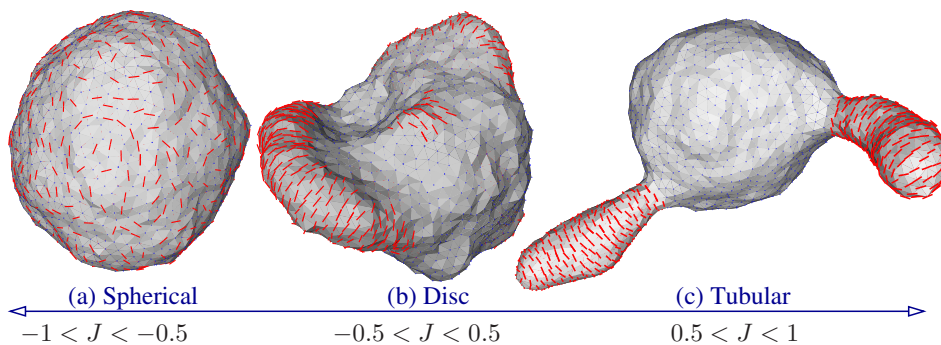


FIG. 2: Equilibrium membrane conformations, with $\phi_A = 0.3$, $\kappa = 20$, $\kappa_{\parallel} = 5$ and $H_{\parallel}^0 = 0.5$ and $\epsilon_{LL} = 3$, for different range of J .

The effect of concentration is shown in Fig.(3) for surface coverage in the range $\phi_A = 0.1 - 0.7$, which display a series of complex shape deformations connected to different aggregate structures. More details will be discussed in section III G.

The aggregation of membrane nematogens also has a temporal aspect. In Fig.(4) we have shown a Monte Carlo time series, for a membrane coverage of 10% nematogens, to illustrate the sequence of domain formation and membrane curvature induced changes leading to the equilibrium structure. The membrane nematogens in an initial randomly dispersed orientation assemble into smaller orientationally ordered domains mediating the final equilibrium structure. These ordered domains often appear as metastable configurations, which either disperse again due to lateral fluctuations or they will eventually funnel into a equilibrium domain configuration. The Monte Carlo dynamics does not reflect the physical kinetics very well, but is useful in identifying kinetic paths connecting various metastable states that lead to the global minima [44, 45].

The aggregation of membrane inclusions mediated by membrane curvature deformations and fluctuations is not specific for nematogens, but is a more general phenomena for membrane curvature active components. It has been well understood in the framework of models for curvature instabilities [5, 19, 46],

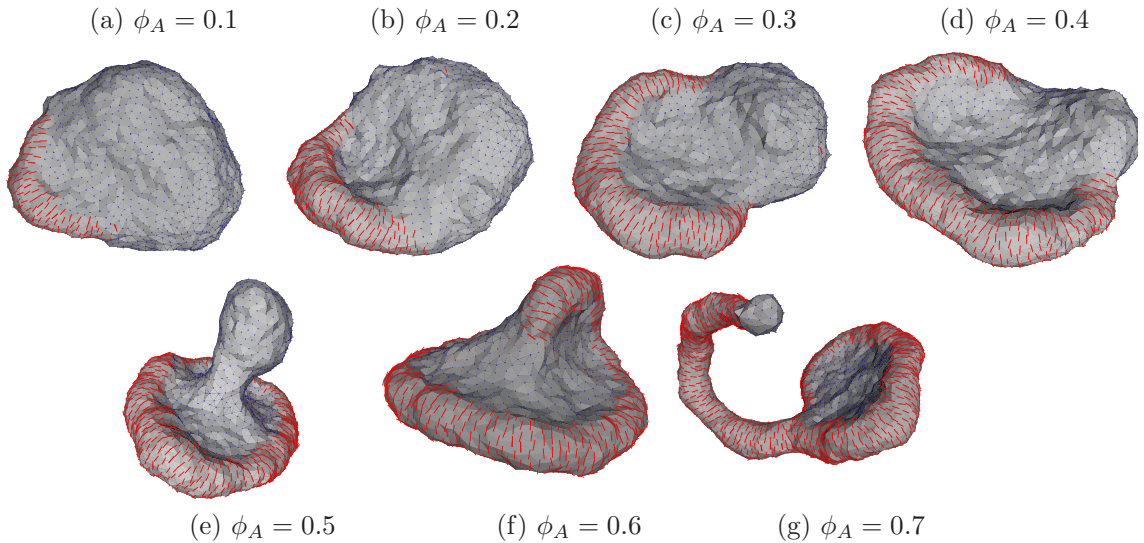


FIG. 3: Equilibrium configurations for varying composition. $\kappa = 10$, $\kappa_{\parallel} = 5$, $\kappa_{\perp} = 0$, $H_{\parallel}^0 = 0.5$, $H_{\perp}^0 = 0$, $J = 0$, $\phi_A = 0.1 - 0.7$ and $\epsilon_{LL} = 3$.

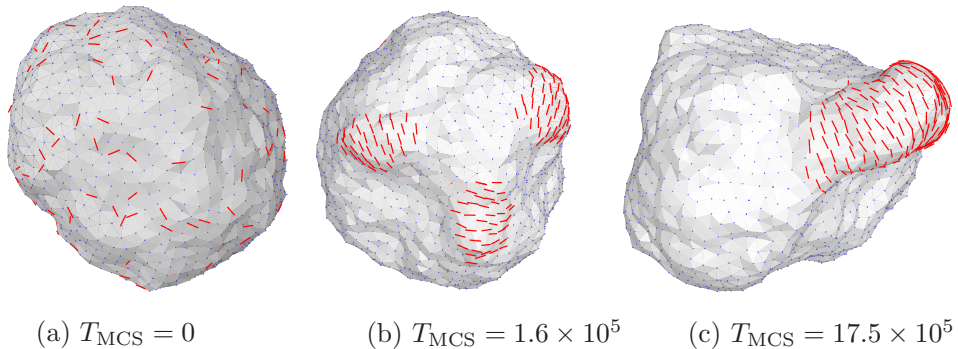


FIG. 4: Aggregation of membrane inclusions for $\kappa = 10$, $\kappa_{\parallel} = 5$, $\kappa_{\perp} = 0$, $H_{\parallel}^0 = 0.5$, $H_{\perp}^0 = 0$, $J = 0$, $\phi_A = 0.1$ and $\epsilon_{LL} = 3$. Monte Carlo time series showing a) random initial configuration of membrane nematogens, b) intermediate state with multiple nematic domains and c) equilibrium conformation where all the small domains coarsen into a single patch.

and has also been demonstrated that simple amphiphathic inclusions, e.g. antimicrobial peptides like Magainin or Melittin [19, 47] and viral membrane active proteins like NSB4 of Hepetites C[48].

The self-association of these membrane components thus needs not to be facilitated by strong direct attractive interaction amongst them. The coupling to the membrane geometry provides additional indirect membrane conformation mediated attractive forces making them to slip into bound structures involving both the proteins and membrane curvature. However, the structure of the aggregates are dependent on the details of the molecular structure and the direct interactions. A general feature of these aggregates is that they appear as nematically ordered domains, where the nematogens form elongated oriented patches with well defined curvature characteristics, e.g. ridges or cylindrical rims. In the following we will in particular focus on the tube-like structures.

B. Tube formation

The most prevalent equilibrium domain structure is the nematic tube, where the membrane protrude into a cylinder like configuration with the membrane nematogens forming a coat around the cylinder. Also for tube formation the overall interaction strength (J) between the membrane nematogens plays a secondary role. It's most pronounced effect is to widen the concentration range for tubulation and to enhance the line tension at the domain boundary, which can induce fission of tubes by narrowing the tube at the boundary of the domain, as in Fig(2(c)). The effect of concentration of membrane nematogens on the membrane tubulation phenomena is shown in Fig.(3(g)). For large concentrations of nematogens or increasing values of J the tubes are the characteristic equilibrium structures shown in Figs. (2,3).

The radius of the equilibrium membrane tubes appears to be relatively well-defined. The radius of the tube with nematic order can be calculated on basis of the continuum model Eq.(5) for the chosen model parameters (see **Supplementary Material**):

$$\bar{r} = \begin{cases} \frac{1}{|H_{0\parallel}|} \sqrt{\frac{\kappa_{\parallel} + \kappa}{\kappa_{\parallel}}} & \text{for } \kappa_{\perp} = 0 \\ \frac{1}{|H_{0\perp}|} \sqrt{\frac{\kappa_{\perp} + \kappa}{\kappa_{\perp}}} & \text{for } \kappa_{\parallel} = 0 \end{cases} \quad (5)$$

So, the radius \bar{r} is set by the curvature elastic model parameters, involving the absolute value of the directional spontaneous curvatures, modulated by the curvature elastic constants. It follows from Eq.(5) that the actual tube radius is somewhat larger than the inverse directional spontaneous curvatures and dependent on the relative strength of the elastic constants.

In experimental systems the membrane tube dimensions can vary considerably with different types of proteins in the cell[1]. Membrane tubes formed *in vitro* by curvature active proteins also display a considerable variability in size. Frost et al. [41] have studied the effect of a number of mutants of CIP4 F-BAR on liposomes. By mutations they find a big variations of tube diameters in the range of 50 to 100 nm.

Membrane tubes induced by membrane inclusions are common phenomena in biological cells, both as more static structures like T-tubules of the muscle cells[24] or more temporal structures like sorting endosomes [49]. The examples shown in Fig.(2,3) corresponds to the cases where spontaneous curvatures are positive, like that induced when F- BAR-domain proteins bind to organelle membranes. However, if the proteins induce negative spontaneous curvatures, as in I-BAR domain proteins, it gives rise to tubular invaginations as shown in Fig.(5) .

As can be seen from Fig.(5), for proteins with large negative spontaneous directional curvatures, at low concentration ($\phi_A = 0.1 - 0.3$), we obtain tubes growing into the interior of the vesicle. As ϕ_A increases, tubes disappear and saddle like regions appear. The inner tubes and saddle like regions coexist again for large concentrations $\phi_A > 0.8$.

C. Protein lattices

Membrane nematogens organize as nematically ordered domains and coat around the membrane to form tubes. Nematogens orient perpendicular to the tube axis when $\kappa_{\perp} = 0, \kappa_{\parallel} \neq 0$ and $H_{\parallel}^0 > 0$. Similarly, $\kappa_{\parallel} = 0, \kappa_{\perp} \neq 0$ and $H_{\perp}^0 \neq 0$ leads to an arrangement of the nematogens along the tube direction. For the common membrane nematogen both these parameters are non-vanishing. Such a case is shown in Fig.(6).

The helical arrangement of the membrane nematogens at the tube surface can be easily understood considering that in general such arrangement will give rise to a global nematic ordering of the membrane nematogens (generalized spirals are the only geodesic curves on long tubes) and the radius is set by the elastic terms. The coupled expressions for the mean values for tube radius \bar{r} and the angle $\bar{\varphi}$ between the tube direction and the nematogen orientation, for different regimes of the dimension less parameter $\tilde{\psi}$:

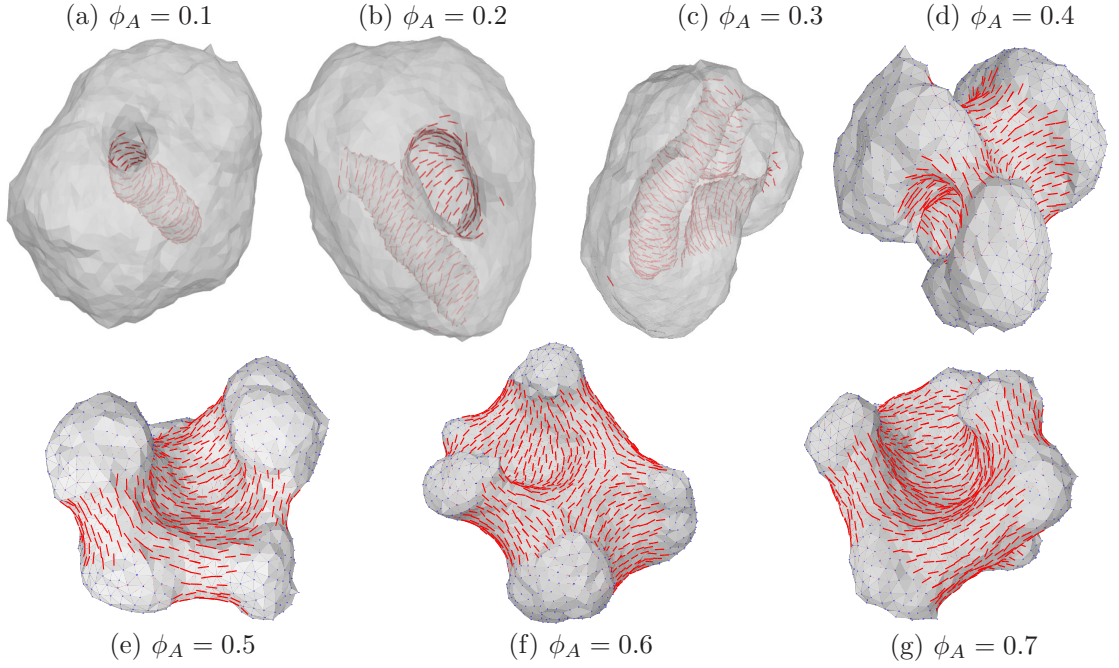


FIG. 5: Equilibrium configurations for vesicle with negative spontaneous curvatures. $\kappa = 10$, $\kappa_{\parallel} = 5$, $\kappa_{\perp} = 0$, $H_{\parallel}^0 = -0.5$, $H_{\perp}^0 = 0.0$, $J = 0$ and $\phi_A = 0.1 - 0.7$.

$$\bar{r} = \begin{cases} \sqrt{\frac{\kappa_{\perp} + \kappa}{\kappa_{\parallel}(H_{\parallel}^0)^2 + \kappa_{\perp}(H_{\perp}^0)^2}} & \text{for } \tilde{\psi} \leq 0, \\ \sqrt{\frac{\left(\frac{\kappa}{2}\right)(\kappa_{\parallel} + \kappa_{\perp}) + \kappa_{\perp}\kappa_{\parallel}}{\kappa_{\perp}\kappa_{\parallel}(H_{\parallel}^0 + H_{\perp}^0)^2}} & 0 < \tilde{\psi} < 1 \\ \sqrt{\frac{\kappa_{\parallel} + \kappa}{\kappa_{\parallel}(H_{\parallel}^0)^2 + \kappa_{\perp}(H_{\perp}^0)^2}} & \tilde{\psi} \geq 1 \end{cases} \quad (6)$$

The parameter $\tilde{\psi}$ is given by the model parameters as:

$$\tilde{\psi} = \frac{\kappa_{\parallel}H_{\parallel}^0 - \kappa_{\perp}H_{\perp}^0}{|H_{\parallel}^0 + H_{\perp}^0|(\kappa_{\parallel} + \kappa_{\perp})} \sqrt{1 + \frac{\kappa}{2} \left(\frac{1}{\kappa_{\parallel}} + \frac{1}{\kappa_{\perp}} \right) + \frac{\kappa_{\perp}}{\kappa_{\parallel}}} \quad (7)$$

similarly for the angle $\bar{\varphi}$:

$$\cos^2(\bar{\varphi}) = \begin{cases} 0 & \text{for } \tilde{\psi} \leq 0, \\ \frac{(\kappa_{\parallel}H_{\parallel}^0 - \kappa_{\perp}H_{\perp}^0)\bar{r} + \kappa_{\perp}}{\kappa_{\perp} + \kappa_{\parallel}} & 0 < \tilde{\psi} < 1 \\ 1 & \tilde{\psi} \geq 1 \end{cases} \quad (8)$$

So, in general both $\bar{\varphi}$ and \bar{r} are set by the model parameters. A derivation of the above expressions are given in **Supplementary Materials**.

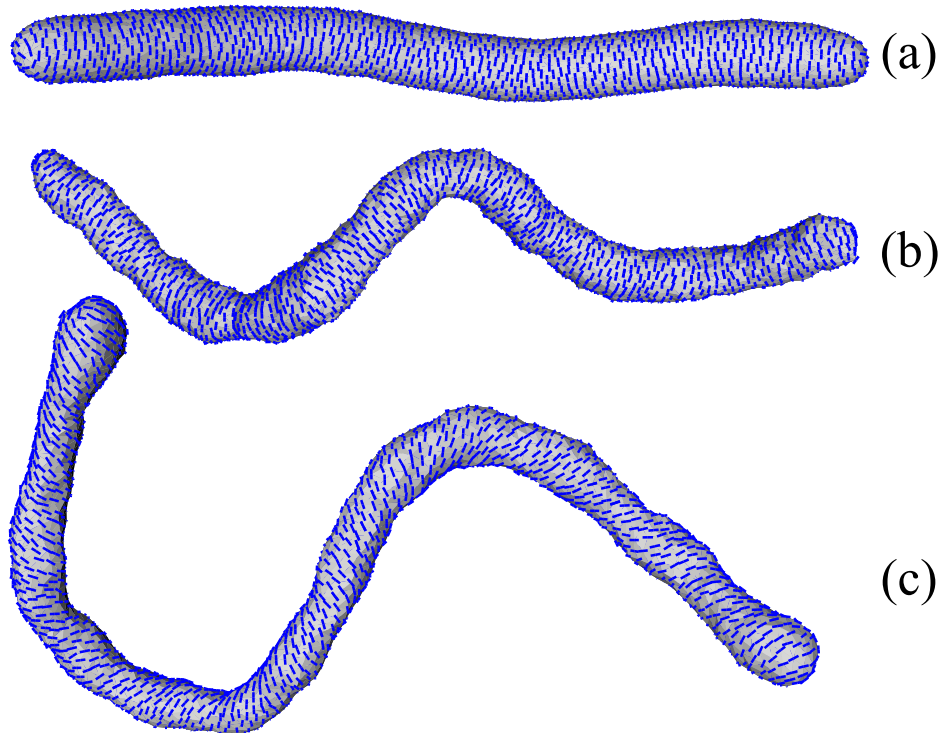


FIG. 6: *Protein lattices*. Modes of a tubular membrane at different state points, for $\kappa = 10$ and $\epsilon_{LL} = 3$. (a) Tubular conformation with $\langle\varphi\rangle = 0$ for $\kappa_{\parallel} = 5$, $\kappa_{\perp} = 0$, $H_{\parallel}^0 = 0.4$, (b) Spiral modes of the tube with $\langle\varphi\rangle = 0$ seen for $\kappa_{\parallel} = 5$, $\kappa_{\perp} = 0$, $H_{\parallel}^0 = 0.4$, and (c) rearrangement of nematics into spiral modes ($\langle\varphi\rangle \neq 0$) when $\kappa_{\parallel} = 5$, $\kappa_{\perp} = 5$, $H_{\parallel}^0 = 0.4$, $H_{\perp}^0 = 0.25$

The spiral organization of the membrane coating proteins has now been observed for many tubular membrane systems *in vivo* and *in vitro*, e.g for the F-BAR proteins[26, 41]. EM-tomographs of tubules of CIP4 F-BAR on liposomes [41] show a fairly dense packing arrangement in the helical tube. The average tube diameter is around 68 nm and the helical angle is about $\varphi = 40^\circ$. Such arrangements are termed *protein lattices* in the cell biology literature. It is found that the helical angle φ of the *protein lattice* with respect to the tube direction adjusts to the tube diameter such that the directional curvature is about the same. For a similar type of experiment with dynamin[50] the membrane tubes of radius $r \simeq 23\text{nm}$ with densely packed helical dynamin coat was observed with a helical pitch of about 15nm (corresponding to a helical angle $\varphi = 80^\circ$).

Our simulation results suggests that the spiral organization of the protein coat on the tube need not be a result of polymerization as often referred in the literature, but can be a self-assembly process of the curvature active proteins mediated by the membrane. Furthermore, the modelling suggest that these *protein lattices* are not conventional two dimensional lattice structures like polymerized membranes or graphene, but rather two dimensional nematic liquid crystalline structures. In the model there is no terms which can distinguish between a right or left turning helix, i.e. the helical arrangement is the result of a spontaneous symmetry breaking. However, the smallest chiral symmetry breaking contribution to the free energy can favor one of the helical orientations without having an effect on any other parameters.

D. Thermal stability of membrane tubes

While our model parameter determine the mean physical properties of the tubes , e.g. the radius, we expect the tubular membranes to display an elastic response to deformations in its shape and organization of the membrane nematogens. This can, for e.g., be reflected in the variation of the shape characteristics due to thermal fluctuations. For analysis of such deformations the continuum description of coated

membrane tubes are suitable and the details can be found in **Supplementary Material**. It is shown that in general the deviations in the orientation of the membrane nematogen and the tube radius are strongly correlated. The thermally induced fluctuations in the radius is found to be

$$\frac{\langle(\delta r)^2\rangle}{\bar{r}^2} = \frac{k_B T}{4\pi} \frac{\kappa_{\parallel} + \kappa_{\perp}}{\kappa_{\parallel}\kappa_{\perp} + (\kappa_{\parallel} + \kappa_{\perp})\frac{\kappa}{2}} \quad \text{for } 0 < \bar{\psi} < 1, \quad (9)$$

where \bar{r} and $\bar{\varphi}$ are respectively the equilibrium tube radius and nematic orientations and $\bar{\psi} = \cos^2 \bar{\varphi}$. We note that the relative variance in r has an upper limit $\frac{k_B T}{2\pi\kappa}$. With a typical range $\kappa \sim 20 - 50k_B T$ this ratio in Eq.(9) is of the order 0.01. For CIP4 F-BAR, reconstituted on liposomes, cryo-tomography measurements give $\bar{r} = 33\text{nm}$ and $\langle(\delta r)^2\rangle/\bar{r}^2 \simeq 0.01$ [41]. If this observed variation in tube thickness is interpreted as frozen in thermal variations, it is in agreement with the the above theory. For rigid membranes with large κ and/or large $\kappa_{\parallel}, \kappa_{\perp}$ values we can consider the thermal excited variations in r as small. Similarly, we can estimate the thermal fluctuations around $\cos^2(\bar{\varphi})$ for such a segment as,

$$\langle(\delta \cos^2(\varphi))^2\rangle = \frac{k_B T}{4\pi} \frac{\kappa_{\parallel}\psi^2 + \kappa_{\parallel}(1 - \psi)^2 + \frac{\kappa}{2}}{\kappa_{\parallel}\kappa_{\perp} + (\kappa_{\parallel} + \kappa_{\perp})\frac{\kappa}{2}} \quad \text{for } 0 < \bar{\psi} < 1. \quad (10)$$

To our knowledge no experimental reports on the random variations in the helical angle has been given. A third type of deformation to consider is the bending of the tubes. It is shown in **Supplementary Materials** that when r is a constant along the tube, the free energy expression is relatively simple. In particular we find that the free energy of bending for a tubular membrane takes the approximate form,

$$\Delta F_{\text{tot}} \approx \frac{1}{2} k_B T l_P \int_0^L ds \lambda(s)^2, \quad (11)$$

where s is the the arc length and $\lambda(s)$ is the line curvature along the tube, while l_P is the persistence length of the tube:

$$l_P = \frac{\pi \bar{r} (K_A + \kappa + \kappa_{\parallel}(1 - \bar{\psi})^2 + \kappa_{\perp} \bar{\psi}^2)}{k_B T}. \quad (12)$$

There are few experimental measurements of the persistence length of membrane tubes with *protein lattices*. For the F-BAR FBP17 producing tubes of radius $r(\text{FBP17}) = 34\text{nm}$ the persistence length was measured to $l_P(\text{FBP17}) = 142\mu\text{m}$ [41] while for amphiphysin $r(\text{amph}) \sim 7\text{nm}$ [51] and $l_P(\text{amph}) = 9\mu\text{m}$ while for dynamin $r(\text{dynamin}) \simeq 20\text{nm}$ and $l_P(\text{dynamin}) = 37\mu\text{m}$. A calculations of l_P from Eq.(12) solely based on κ gives predictions which are an order of magnitude too small, which indicates that other elastic constants $\kappa_{\parallel}, \kappa_{\perp}$ and K_A gives the main contributions to l_P .

E. Capping the tubes, Defects

The formation of membrane tubes with helical coats seems to be generic for systems with membranes with membrane nematogens. Either the helical coat has to terminate resulting in an interfacial curve separating the coated and uncoated regions or the vesicle should sprout tubes and buds with the tips having a pair of point defects. The way this takes place in the tube end or at a domain boundary is mainly determined by the competition between interfacial tension, which in our model is largely regulated by the parameter J , and bending modulus. In Fig(7) is shown that when the interaction parameter J is increased the interfacial line shrinks, first transforming the vesicle from a disk to a structure with partially coated tubes and buds, but still no defects. Further increase in the line tension will result in tubes and buds that are fully coated but minimizing the length of the interfacial line between coated and uncoated regions. It does so by either moving the interfaces to the end of the tube forming a pair of point defects or deforming the membrane to form a narrow neck. Note that the line does not shrink to a single point defect of strength +1 but instead forms a pair of +1/2 defects bound to each other. This is the result of of the π symmetry of the membrane nematogen and the strong coupling between membrane curvature and nematic orientation [52–54]. To our knowledge no details about the capping of the coated membrane tubes have been provided by experiments.

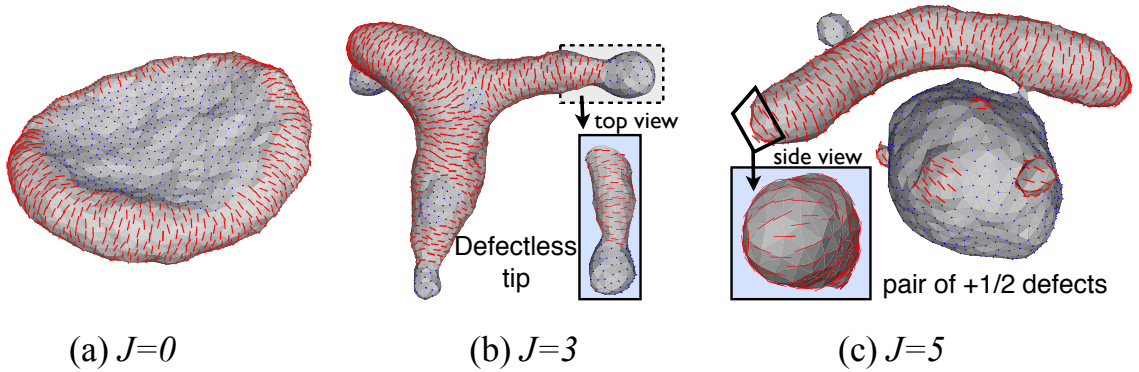


FIG. 7: A partly decorated membrane with $\kappa = 20$, $\kappa_{\parallel} = 5$, $\epsilon_{LL} = 3$. Shown are: (a) a disc without a defect for $\phi_A = 0.4$, $H_{\parallel}^0 = 0.5$ and $J = 0$. (b) Tubes without defects at $J = 3$. (the bottom panel shows an enlarged side view of the tip of a tube without defects). (c) Tubes and buds with defects when $J = 5$. (the bottom panel shows an enlarged top view of the tip of a bud with defects)

F. Curvature differences leads to segregation

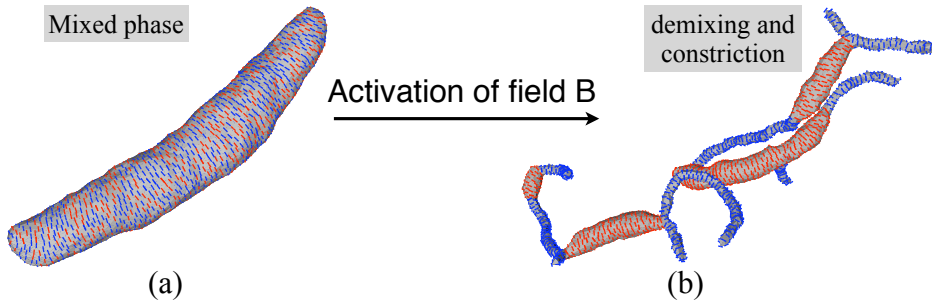


FIG. 8: (a) Tubular membrane of uniform cross section with fields A and B in the mixed phase for $H_{\parallel,A}^0, H_{\parallel,B}^0 = 0.5, 0.5$. (b) Activation of field B takes $H_{\parallel,B}^0$ from 0.5 to 1.25. The difference in the spontaneous curvatures leads to phase segregation and results in the constriction of tubes. Field concentrations are respectively $\phi_A = 0.4$ and $\phi_B = 0.6$ while $\kappa = 10k_B T$, $\kappa_{\parallel}^A = \kappa_{\parallel}^B = 5k_B T$ and $\epsilon_{AA} = \epsilon_{BB} = 3k_B T$.

Another example of the curvature driven aggregation is demonstrated in Fig. 8. Shown in Fig. 8(a) is a tubular membrane of uniform cross section, fully decorated by two different types of membrane nematogens, labelled A and B. The tube is stable, in the mixed state, when the directional spontaneous curvature of the in-plane fields, $H_{\parallel,A}^0 = H_{\parallel,B}^0 = 0.5$, are the same. If a source of activation increases the spontaneous directional curvature of B to $H_{\parallel,B}^0 = 1.25$, analogous to activation of dynamin proteins by hydrolysis of GTP, the fields demix. The regions containing field B constrict the tube further. The equilibrium shape of the activated membrane is observed to have successive tubular regions of large and small curvatures (see Fig. 8(b)), similar to the striated patterns of dynamin tubes obtained on treatment with GTP γ S [55, 56]. For dynamin the molecular conformation and membrane tube diameter is GTP dependent [56, 57]. Furthermore it is observed that the tube constriction involves a tube twisting, suggesting a change in the helical angle φ [58]. In *in vivo* experiments, it has been demonstrated that structurally similar F-BAR proteins can co-localize into the same membrane tubes [14] while differing BAR proteins, like F-BAR and N-BAR, segregate into separate membrane tubes with their respective characteristic r and φ [41, 59]. Our analysis suggests that this recruitment of differing BAR-proteins into separate domains is possibly driven by their directional spontaneous curvatures.

G. Sheets versus tubes

The effect of concentration, shown in Fig.(3), for surface coverages in the range 10% and 70% display a series of complex shape deformations connected to different aggregate structures. The regime, where inclusions stay separate, for the model parameters chosen here, appear at very low concentrations. The figure illustrates that for a system where the direct interactions parameter J between the membrane nematogens are weak the oligomers tend form larger rim-like formations, which stabilizes disc like structures of vesicles. The rims form the edges of the discs. As the concentration is increased part of the edge turn tubular.

So for a range of concentrations the disc and the tubes coexist. The tubules get more pronounced and the discs diminishes with the increase in concentration of membrane nematogens. Recent experiments on the formation of tubular (or smooth) ER suggest that some membrane curvature active proteins, reticulon protein and DP1[15], are highly enriched in the tubular ER [60] and the ER sheet edges[16]. Our results are thus in line with the idea that the concentration of these membrane nematogens are a major determinant for the amount of ER in sheets or tubules[16].

IV. CONCLUSION

We have described the membrane curvature modifying properties of anisotropic protein inclusions, like the BAR proteins, in terms of an in-plane nematic field. We have shown that the flexibility of the membrane can promote aggregation and lateral domain formation of these membrane nematogens, even in the absence of self interactions. These domains can facilitate shape changes of the membrane. The equilibrium shapes obtained are strikingly similar to that seen in experiments involving curvature modifying proteins. Prominent structures seen are tubes and discs and coexistence of them. Depending on the preferred curvature of the nematogens, a *protein lattice* with helical nematic orientation around the tube is seen. The properties of this liquid crystalline structure was further analyzed from a continuum version of the model and the dependence of the tube radius and the orientation of the nematic with respect to the tube axis was calculated. We also estimate the thermally induced fluctuation in these quantities and show that they are comparable to what is seen in experiments. In addition we calculate the persistence length of the nematogen induced tubes and show that it is in the range of experimentally obtained values. This analysis provides the necessary basis to obtain estimates of model parameters from experiments on coated membrane tubes. At present the available experimental data are very limited.

The present modeling provides additional support to the growing notion of the importance of local curvature modulating proteins in membrane shape generation in biological cells. Compared to previous modeling of the role of membrane proteins inducing directional membrane curvature we have taken into account that membranes are not fully decorated, the in-plane interactions between nematogens and the arbitrary membrane shapes with spherical topology. The current work focusses only on the membrane interacting part of the protein. Electric charges in BAR-protein are mostly localized to its membrane facing domain which in turn interact with anionic lipids and enables them to bind strongly to the membrane. One natural extension of this model is include the electrostatic interactions through cytosol between proteins moieties protruding out of the membrane.

We emphasize that the main aim of this work is to show that anisotropic curvature induced by the inclusions can lead to aggregation and interesting shape changes. This is in contrast to the prevailing assumption that explicit protein interactions are essential for aggregation and formation of protein lattices. Though a quantitative comparison between the predictions of this model and experiments is not so easy, the model does demonstrate the possibility of generating many biologically relevant shapes of the vesicle by membrane mediated interactions alone.

V. ACKNOWLEDGEMENTS

The computational work is carried out at HPC facility at IIT-Madras.

-
- [1] Frost A., V.M. Unger, and P. De Camilli, 2009, The BAR Domain Superfamily: Membrane-Molding Macromolecules. *Cell* 137, 191-196.
 - [2] Opaliński L., Kiel J. A.K.W., C. Williams, M. Veenhuis, and I.J. van der Klei, 2011, Membrane curvature during peroxisome fission requires Pex11. *The EMBO Jour.* 30, 5.
 - [3] Antony B, 2006, Membrane deformations by protein coats. *Curr. Opinion in Cell Biol.* 18, 386.
 - [4] Sackmann E., R. Kotulla, and F-J. Heiszler, 1984, On the role of lipid-bilayer elasticity for the lipid-protein interaction and the indirect protein-protein coupling. *Canadian Jour. of Biochem. and Cell Biol.* 62, 778
 - [5] Leibler S., 1986, Curvature instability in membranes. *J. Phys. France* 47, 507-516.
 - [6] Ramakrishnan N, P.B. Sunil Kumar, J.H. Ipsen, 2010, Monte Carlo simulations of fluid vesicles with in-plane orientational ordering. *Phys. Rev. E* 81, 041922.
 - [7] Peter B.J., H.M. Kent, I.G. Mills, Y. Vallis, P.J.G. Butler, P.R. Evans and H.T. McMahon, 2004, BAR Domains as Sensors of Membrane Curvature: The Amphiphysin BAR Structure. *Science* 303, 495-499.
 - [8] Weissenhorn W., 2005, Crystal structure of the Endophilin-A1 BAR Domain. *J. Mol. Biol.* 351, 653-661.
 - [9] McMohan H.T. and J. L. Gallop, 2005, Membrane curvature and mechanisms of dynamic cell membrane remodelling. *Nature* 438, 590-596.
 - [10] Blood P.D. and G.A. Voth, 2006, Direct observation of Bin/amphiphysin/Rvs (BAR) domain-induced membrane curvature by means of molecular dynamics simulations *Proc. Natl. Acad. Sci.* 103, 15068-15072
 - [11] Arkhipov A., Y. Ying, and K. Schulten, 2008, Four-scale description of membrane sculpting by BAR domains. *Biophys. J.* 95, 2806-2821,
 - [12] Shnyrova A.V., V. A. Frolov and J. Zimmerberg, 2009, Domain-Driven Morphogenesis of Cellular Membranes. *Current Biology* 19, R772-R780.
 - [13] Williams T.M. and M.P. Lisanti, 2004, The caveolin proteins. *Genome Biology* 5,214,1-8.
 - [14] Shimada A, H. Niwa, K. Tsujita, S. Suetsugu, K. Nitta, K. Hanawa-Suetsugu, R. Akasaka, Y. Nishino, M. Toyama, L. Chen, Z.J. Liu, B.C. Wang, M. Yamamoto, T. Terada, A. Miyazawa, A. Tanaka, S. Sugano, M. Shirouzu, K. Nagayama, T. Takenawa, S. Yokoyama, 2007, Curved EFC/F-BAR-domain dimers are joined end to end into a filament for membrane invagination in endocytosis. *Cell* 129, 761-72.
 - [15] Voeltz G.K., W.A. Prinz, Y. Shibata, J.M. Rist and T.A. Rapoport, 2006, A class of membrane proteins shaping the tubular endoplasmatic reticulum, *Cell* 124, 573-586.
 - [16] Shibata Y., T. Shemesh, W.A. Prinz, A.F. Palazzo, M.M. Kozlov and T.A. Rapoport, 2010, Mechanisms Determining the Morphology of the Peripheral ER. *Cell* 143, 774-788.
 - [17] Farsaq K., N. Ringstad, K. Takei, S.R. Floyd, K. Rose, and P. De Camilli, 2001, Generation of high-curvature membranes mediated by direct endophilin bilayer interactions. *J. Cell Biol.* 155, 193-200.
 - [18] Gallop J. L., C.C. Jao, H.M. Kent, J.G. Butler, P.R. Evans, R. Langen and H.T. McMahon, 2006, Mechanism of endophilin N-BAR domain mediated membrane curvature. *The EMBO Journal* 25, 2898-2910.
 - [19] Bouvrais H., K. J. Jensen, J. Brask, P. Méléard, T. Pott and J.H. Ipsen, 2008, Softening of POPC membranes by Magainin. *Biophysical Chemistry* 137 7-12.
 - [20] Campelo F., McMahon H.T and M.M. Kozlov, 2008, The hydrophobic insertion mechanism of membrane curvature generation by proteins *Biophys. J.* 95, 2325-2339
 - [21] Kurten R.C., A.D. Eddington, P. Chowdhury, R.D. Smith, A.D. Davidson and B.B. Shank, 2001, Self-assembly and binding of a sorting nexin to sorting endosomes. *J. Cell Science* 114, 1743-1756.
 - [22] Mayor S., J.F. Presley and F.R. Maxfield, 1993, Sorting of Membrane Components from Endosomes and Subsequent Recycling to the Cell Surface Occurs by a Bulk Flow Process. *J. Cell. Biol.* 121,1257-1269.
 - [23] Shepard, K.A. and M.P. Yaffe, 1999, The Yeast Dynamin-like Protein, Mgm1p, Functions on the Mitochondrial Outer Membrane to Mediate Mitochondrial Inheritance. *J. Cell. Biol.* 144, 711-720.
 - [24] Razaq A., I.M. Robinson, H.T. McMahon, J.N. Skepper, Y. Su1, A.C. Zehhof, A.P. Jackson, N.J. Gay and C.J. O’Kane, 2001, Amphiphysin is necessary for organization of the excitation contraction coupling machinery of muscles, but not for synaptic vesicle endocytosis in *Drosophila*. *Genes & Dev.* 15, 2967-2979
 - [25] Sweitzer S.M. and J.E. Hinshaw, 1998, Dynamins Undergoes a GTP-Dependent Conformational Change Causing Vesiculation. *Cell* 98, 1021-1029.
 - [26] Low H.H., C. Sachse, A.A. Amos, and J. Löwe, 2009, Structure of a Bacterial Dynamin-like Protein Lipid Tube Provides a Mechanism For Assembly and Membrane Curving. *Cell* 139, 1342-1352.
 - [27] Lebbink M.N., N. Jiménez, K. Voeking, L.H. Hekking, A.J. Verkleij and J.A. Post. 2010. Spiral Coating of the Endothelial Caveolar Membranes as Revealed by Electron Tomography and Template Matching. *Traffic* 11, 138-150.
 - [28] Sens P. and M. S. Turnery, 2004, Theoretical Model for the Formation of Caveolae and Similar Membrane

- Invaginations. *Biophys. J.* 86, 2049-2057.
- [29] Fournier J. -B., 1996, Nontopological saddle-splay and curvature instabilities from anisotropic membrane inclusions. *Phys. Rev. Lett.*, 76(23), 4436.
- [30] Fournier J. -B. and P. Galatola, 1998, Bilayer Membranes with 2D-Nematic Order of the Surfactant Polar Heads. *Braz. Jour. of Phys.*, 28, 329.
- [31] Krajc-Iglic V., V. Heinrich, S. Svetina, S. and B. Zeks, 1999, Free energy of closed membrane with anisotropic inclusions. *Eur. Phys. J. B* 10, 5-8.
- [32] Dommersnes P. G. and J.-B. Fournier, 1999, N-body study of anisotropic membrane inclusions: Membrane mediated interactions and ordered aggregation *Eur. Phys. J. B* 12, 9-12.
- [33] Iglic A., T. Slivnik, and V. Krajc-Iglic, 2007, Elastic properties of biological membranes influenced by attached proteins. *J. Biomech.* 40, 2492-2500.
- [34] Helfrich W., 1973, Elastic properties of lipid bilayers: theory and possible experiments. *Naturforsch. Z.* 28, 693-703.
- [35] Onsager L., 1949, The effects of shape on the interaction of colloidal particles. *Annals of the New York Academy of Sciences* 51, 627-659.
- [36] Park J.-M and T. C Lubensky, 1996, Interactions between membrane Inclusions on Fluctuating Membranes. *Journal de Physique I* 6, 1217.
- [37] Kim K. S., J. Neu, and G. Oster, 1998, Curvature-mediated interactions between membrane proteins. *Biophys. J.* 75, 2274.
- [38] Chou T., K. S. Kim and G. Oster, 2001, Statistical thermodynamics of membrane bending-mediated protein-protein attractions. *Biophys. J.* 80, 1075.
- [39] Lewandowski, E. P., J. A. Bernate, P. C. Searson, P. C and K. J. Stebe, 2008, Rotation and Alignment of Anisotropic Particles on Nonplanar Interfaces, *Langmuir*, 24, 9302.
- [40] Lewandowski, E. P., J. A. Bernate, A. Tseng, P. C. Searson, P. C and K. J. Stebe, 2009, Oriented assembly of anisotropic particles by capillary interactions, *Soft Matter*, 5, 886.
- [41] Frost A., R. Perera, A. Roux, K. Spasov, O. Destaing, E.H. Engelmann, P. De Camilli, and A. Unger, 2008, Structural Basis of Membrane Invaginations by F-BAR Domains. *Cell* 132, 807-817.
- [42] Peliti L. and J. Prost, 1989, *J.Phys. France* 50, 1557-1571.
- [43] Frank J. R. and M. Kardar, 2008, Defects in nematic membranes can buckle into pseudospheres, *Phys. Rev. E* 77, 041705.
- [44] Kumar P. B. S. and Madan Rao, 1998, Shape Instabilities in the Dynamics of a Two-Component Fluid Membrane, *Phys. Rev. Lett.* 80, 2489.
- [45] Kumar P. B. S., Gerhard Gompper and Reinhard Lipowsky, 2001, Budding Dynamics of Multicomponent Membranes, *Phys. Rev. Lett.* 86, 3911.
- [46] Henriksen J.R., T.L. Andresen, L. Feldborg, L. Duelund, and J.H. Ipsen, 2010, Understanding Detergent Effects on Lipid Membranes: A Model Study. *Biophys. J.* 98, 2199-2205.
- [47] Gerbeaud C, 1998, Effect de l'insertion de protéines et de peptides membranaires sur les propriétés mécaniques et les changements morphologiques de vésicules géantes. *Ph.d. thesis L'Université Bordeaux I.*
- [48] Gouttenoire J., P. Roingeard, F. Penin, and D. Moradpour1, 2010, Amphipathic α -Helix AH2 Is a Major Determinant for the Oligomerization of Hepatitis C Virus Nonstructural Protein 4B. *Journal of Virology* 84, 12529-12537.
- [49] Bonifacino J.S. and J.H. Hurley, 2008, Retromer, *Curr. Opinion in Cell Biol.* 20, 427-436
- [50] Sweitzer S.M. and J.E. Hinshaw, 1998, Dynamin undergoes a GTP-dependent conformational change causing vesiculation. *Cell* 93, 1021.
- [51] Sorre B, A. Callan-Jones, J. Manzi, B. Goud, J. Prost, P. Bassereau, A. Roux, 2012, Nature of curvature coupling of amphiphysin with membranes depends on its bound density. *Proc. Natl. Acad. Sciences* 109, 173-8.
- [52] Lubensky T.C. and J. Prost, 1992, Orientational order and vesicle shape. *J. Phys. France II* 2, 371-382.
- [53] Vitelli V. and D.R. Nelson, 2004, Defect generation and deconfinement on corrugated topographies. *Phys. Rev. E* 70, 051105.
- [54] Ramakrishnan N., J. H. Ipsen, P. B. Sunil Kumar, 2012, Role of disclinations in determining the morphology of deformable fluid interfaces. *Soft Matter* 8, 3058-3061.
- [55] Roux, A., G. Koster, M. Lenz, B. Sorre, J.-B. Manneville, P. Nassoy and P. Bassereau, 2010, Membrane curvature controls dynamin polymerization. *Proc. Natl. Acad. Sciences* 107, 4141-4146.
- [56] Danino D., K-H. Moonb and J.E. Hinshaw, 2004, Rapid constriction of lipid bilayers by the mechanochemical enzyme dynamin. *Journal of Structural Biol.* 147, 259-267.
- [57] Zhang P. and J.E. Hinshaw, 2001, Three-dimensional reconstruction of dynamin in the constricted state. *Nature Cell Biology* 3, 922-926.
- [58] Roux A., K. Uyhazi, A. Frost, and P. De Camilli, 2006, GTP-dependent twisting of dynamin implicates constriction and tension in membrane fission. *Nature* 44, 528-531.
- [59] Itoh T. and P. De Camilli, 2006, BAR, F-BAR(EFC), and ENTH/ANTH domains in the regulation of membrane cytosol interfaces and membrane curvature. *Biochim. Biophys. Acta* 1761, 897-912

- [60] Shibata Y., C. Voss, J.M. Rist, J. Hu, T.A. Rapoport, W.A. Prinz and G.K. Voeltz, 2008, The reticulon and DP1/Yop1p proteins form immobile oligomers in the tubular endoplasmic reticulum. *J. Biol. Chem.* 283, 18892-904.